Environmental Modelling & Software 24 (2009) 1073–1087

Contents lists available at ScienceDirect

Environmental Modelling & Software

journal homepage: www.elsevier.com/locate/envsoft

Assessment of nitrate contamination of groundwater using lumped-parameter models

Lubna Hajhamad, Mohammad N. Almasri*

College of Engineering, Department of Civil Engineering, An-Najah National University, P.O. Box 7, Nablus, Palestine

ARTICLE INFO

Article history:
Received 30 March 2008
Received in revised form
20 February 2009
Accepted 23 February 2009
Available online 24 March 2009

Keywords:
Nitrate
Groundwater
Contamination
Modeling
Management
Palestine

ABSTRACT

In this paper, lumped-parameter models (LPMs) were developed and utilized to simulate nitrate concentration in the groundwater of Gaza City and Jabalia Camp (GCJC) in the Gaza Coastal Aquifer (GCA) in Palestine. In the GCJC area, nitrate levels exceed the maximum contaminant level (MCL) of 10 mg/L NO_3-N (45 mg/L NO_3) in many wells. Elevated nitrate concentrations in the groundwater of GCJC area are due to the disposal of untreated wastewater, the existence of heavy agriculture in the surrounding areas, and the use of cesspits for wastewater disposal. The developed LPMs utilize monthly time steps and take into consideration all the sources and sinks of water and nitrate in the study area. The main outcomes of the LPMs are the average temporal water table elevation and nitrate concentration. In order to demonstrate LPMs usability, a set of management options to reduce nitrate concentration in the groundwater of the study area were proposed and evaluated using the developed LPMs. Four broad management options were considered where these options tackle the reduction of nitrate concentration in the lateral inflow, rehabilitation of the wastewater collection system, reduction in cesspit usage, and the restriction on the use of nitrogen-based fertilizers. In addition, management options that encompass different combinations of the single management options were taken into account. Different scenarios that correspond to the different management options were investigated. It was found based on the LPMs that individual management options were not effective in meeting the MCL of nitrate. However, the combination of the four single management options with full rehabilitation and coverage of the wastewater collection network along with at least 60% reduction in both nitrate concentration in the lateral inflow and the use of nitrogen-based fertilizers would meet the MCL constraint by the end of the management period.

1. Introduction

Many regions all over the world depend entirely on groundwater resources for various uses (Babiker et al., 2003; Thirumalaivasan et al., 2003). However, the population growth and the increase in demand for water and food supplies place an increasing stress on the groundwater quantity and quality (Joosten et al., 1998; Lewis and Bardon, 1998; Thirumalaivasan et al., 2003; De Santa Olalla et al., 2007; Tait et al., 2008) where over-abstraction depletes the available quantity of groundwater (Ataie-Ashtiani, 2007). In addition, the increase in demand for food supplies may lead to groundwater contamination by nitrate since the major contributor to nitrate contamination in groundwater is the use of nitrogen-based fertilizers associated with cropping activities (Konikow and Person, 1985; Shamrukh et al., 2001; Wolf et al., 2003; Almasri and Kaluarachchi, 2005; Mao et al., 2006; Tait et al., 2008). Elevated nitrate concentrations in drinking water can cause methemoglobinemia in infants and stomach cancer in adults (Lee et al., 1991; Wolfe and Patz, 2002). Because of that the US Environmental Protection Agency (US EPA) has established a maximum contaminant level (MCL) of 10 mg/L NO_3-N (US EPA, 2000).

Sources of groundwater contamination by nitrate can be classified into point and non-point sources. Non-point sources of nitrogen include fertilizers, manure application, leguminous crops, dissolved nitrogen in precipitation, irrigation return-flows, and dry deposition. Point sources such as septic systems and cesspits can also be major sources of nitrate pollution (Joosten et al., 1998; Stournaras, 1998; Mitchell et al., 2003; Babiker et al., 2003; Almasri and Kaluarachchi, 2005; Wolf et al., 2003; Santhi et al., 2006; Tait et al., 2008).

Nitrogen applied through fertilizers or manure is converted to plant-available-nitrate by bacteria living in the soil. The growing plants uptake part of this nitrate. The nitrate that is not taken up by crops, immobilized by bacteria into soil organic matter or converted

* Corresponding author. Tel: +972 9 2394960; fax: +972 9 2345982.
E-mail address: mnmasri@najah.edu (M.N. Almasri).

1364-8152/$ – see front matter © 2009 Elsevier Ltd. All rights reserved.
doi:10.1016/j.envsoft.2009.02.014

to atmospheric gases by denitrification can leach from the root zone and possibly end up in groundwater (Bhumbla, 1999).

Nitrogen-based fertilizers used on a sandy soil have a high potential to cause nitrate to leach to groundwater when compared to a clay soil. Water moves rapidly through sandy or other coarse-textured soils (Kraft and Stites, 2003; Babiker et al., 2003). The negative charge on the clay particles retains ammonium ions, which prevents ammonia from leaching. Nitrate ions are negatively charged and are not retained by the clay particles.

Overall, groundwater contamination has become a major concern in the recent years (Kalivarapu and Winer, 2008). The Gaza Coastal Aquifer (GCA) is characterized by both quantity and quality problems due to the over-abstraction, excessive fertilization and untreated/poorly treated wastewater disposal (Assaf, 2001; Shomar et al., 2006). GCA is an important source of water to almost 1.5 million residents in Gaza Strip and is utilized extensively to satisfy agricultural, domestic, and industrial water demands (Metcalf and Eddy, 2000; UNEP, 2003). The GCA and the overlying soils are composed mainly of sands, which promote the vulnerability of the GCA to contamination through the high potential of nitrate leaching to groundwater. The groundwater that underlies Gaza City and Jabalia Camp (GCJC) is part of GCA and serves about half a million residents (see Fig. 1 for GCJC area). The groundwater of GCJC area represents a typical coastal aquifer where both over-pumping and the high-density population represent major water quantity and quality problems (see for instance Ataie-Ashtiani, 2007).

In order to simulate nitrate contamination in the groundwater of the GCJC area, two lumped-parameter models (LPMs) were developed. LPMs offer the opportunity to simulate a given system with fewer data requirements for parameterization and calibration compared with their distributed counterparts (Ling and El-Kadi, 1998). The literature is packed with studies that utilized LPMs for the analysis of groundwater systems as in Gelhar and Wilson (1974), Mercado (1976), Barrett and Charbeneau (1997), Ling and El-Kadi (1998) and Desbarats (2002). For instance, Mercado (1976) developed a single-cell model to study the regional chloride and nitrate pollution patterns in coastal aquifers. Barrett and Charbeneau (1997) developed an LPM for reproducing general historical trends for groundwater levels. Ling and El-Kadi (1998) developed an analytical LPM for the simulation of nitrate leaching from the unsaturated zone in agricultural areas.

Many of the abovementioned studies did utilize LPMs in assessing the efficacy of management options in remedying a situation. For instance, Mercado (1976) utilized a LPM in examining thirteen alternative protection measures to conserve groundwater quality from nitrate contamination. Such measures include advanced treatment of sewage water prior to their recharge to the aquifer, reduction of fertilizer dosage to crops, and exchange of nitrate-contaminated groundwater by low-nitrate surface waters.

The main objective of this paper is to develop LPMs for the simulation of water table elevation and nitrate concentration for the groundwater of GCJC area. The LPM development is depicted conceptually and mathematically. The developed LPMs consider all sources and sinks of water and nitrate and provide the simulated average nitrate concentration for the GCJC area. The LPMs were utilized for the assessment of the effectiveness of potential management options to mitigate the nitrate contamination problem in the GCJC area.

2. Model development

The mass balance approach was used for both water and nitrate to develop the LPMs. This concept of mass balance implies that the difference between inputs and outputs must equal the change in the storage for the system boundary or model domain (Freeze and Cherry, 1979).

The LPMs are comprised of two key components (models): the quantity (water) and quality (nitrate). Although the development of the nitrate model is the key target, the nitrate model requires the development of the water model and hence two LPMs were utilized. This is because the nitrate concentration over time, $C(t)$, in the aquifer depends on the available water quantity which can only be computed through the simulation of the temporal water table

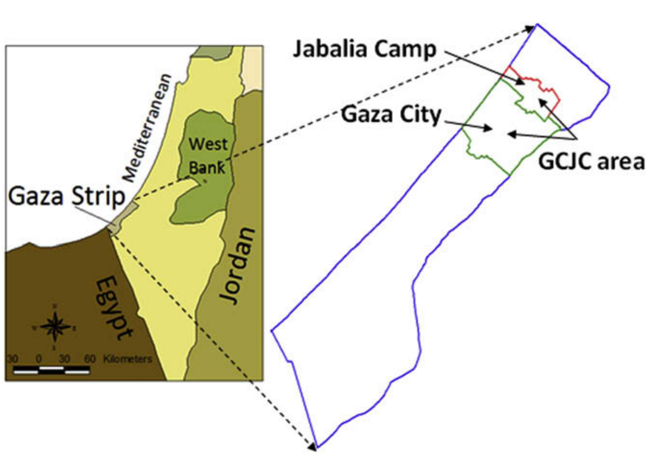

Fig. 1. Regional setting of Gaza Strip along with the location of the GCJC area.

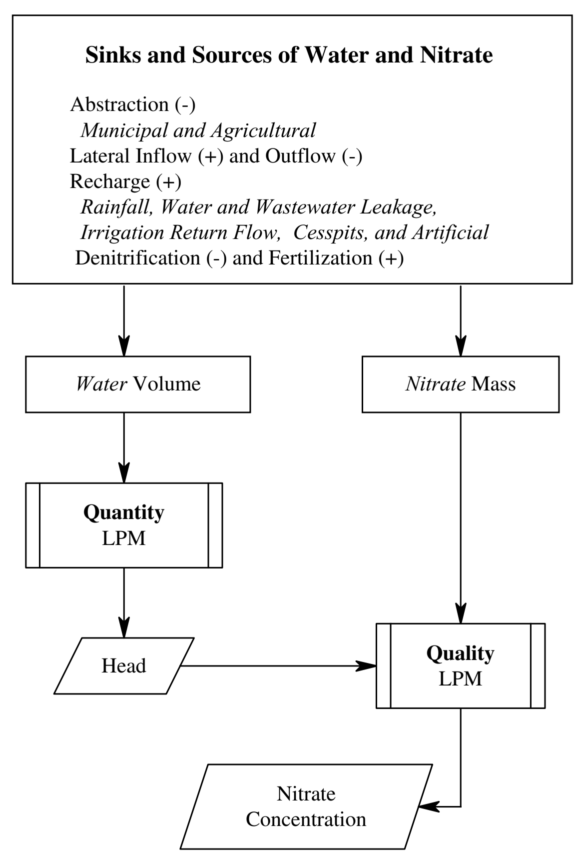

Fig. 2. Schematic of the development of the quantity and quality LPMs along with a depiction of the sinks and sources of water and nitrogen. Signs in brackets indicate the sink (−) and source (+). Note that denitrification and fertilization affect nitrate mass but do not influence the water quantity.

elevation denoted as $h(t)$. Fig. 2 depicts the overall schematic for model development and the main linkage between the water and the nitrate models. Fig. 2 also shows the sinks and sources of water and nitrate considered in the development of the LPMs. The following sections illustrate the development of the conceptual models for water and nitrate.

2.1. Development of the quantity LPM

Fig. 2 depicts the conceptual model development where lateral inflow, artificial recharge, and natural recharge were classified as inputs to the model domain. Lateral outflow and water pumped for irrigation and domestic uses were classified as outputs from the model domain. The details of the parameters of the quantity LPM follow in the subsequent sections. Additional details can be found in Hajhamad (2007).

2.1.1. Lateral inflow

Lateral inflow (G_{in}) is the subsurface flow that enters the model domain from its lateral boundaries and can be computed using Darcy's law. In order to implement Darcy's law, the model boundary was divided into segments as depicted in Fig. 3. Each segment (j) carries a value for hydraulic gradient, width, and saturated thickness. The hydraulic gradient can be computed from the groundwater elevation contour lines after considering the change in the hydraulic head and the perpendicular distance between the contour lines upon which head difference is measured. The saturated thickness of the aquifer is computed by summing up the absolute value of the distance from the sea level to the average bottom of the aquifer (D_p) and the average water table elevation from sea level (WT). The value of WT can be positive or negative. As an approximation for the LPM, D_p was approximated as the weighted average depth to the bottom of the pumping wells

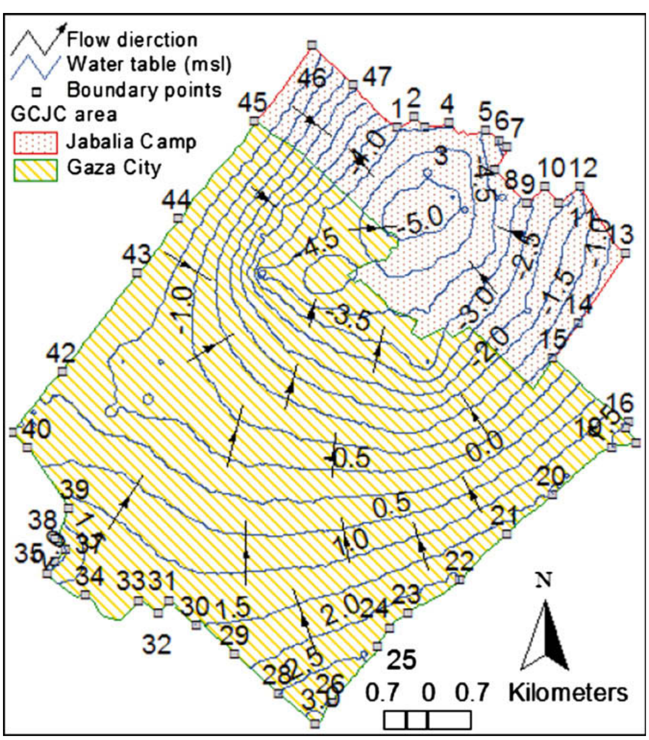

Fig. 3. Water table contours for the study area as for the year 2000 along with the direction of groundwater flow. The figure depicts the segmentation of model boundaries for the computation of lateral inflow and outflow. For instance, segment 1 ($j = 1$) is bounded by points 1 and 2 as shown in the figure.

distributed throughout the study area after considering well depth and pumping rate.

2.1.2. Artificial recharge

Artificial recharge (Q_{Ar}) is the amount of water injected intentionally into the aquifer in order to increase the water table elevation which serves the management objective of mitigating the problem of seawater intrusion in coastal aquifers. Artificial recharge can be also considered for mixing water of good quality with contaminated groundwater to reduce contaminant concentration.

2.1.3. Recharge

In general, total recharge to groundwater equals the summation of recharge from rainfall, irrigation return-flow, wastewater leakage, leakage from water networks, and cesspits as depicted in Fig. 2. Equation (1) was used to compute the overall recharge to the model domain as follows:

$$R = R_{ra} + R_{Ir} + R_{WWL} + R_{WL} + R_{CSPT} \quad (1)$$

where R is the total recharge (L^3/T); R_{ra} is the recharge from rainfall (L^3/T); R_{Ir} is the recharge from irrigation return-flow (L^3/T); R_{WWL} is the recharge from wastewater leakage (L^3/T); R_{WL} is the recharge from water leakage (L^3/T); and R_{CSPT} is the recharge from cesspits (L^3/T). In the following subsections, all the recharge components given in equation (1) are illustrated.

2.1.3.1. Recharge from rainfall. In order to compute the recharge from rainfall for the GCJC area, the locations of rainfall stations were mapped using GIS. A GIS point shapefile of rainfall stations was created based on the spatial coordinates of these stations. For each station, the total monthly rainfall depth was computed based on the available daily values. Thiessen polygons were created for each station using GIS where each transpired polygon was represented by a single station. In order to account for the recharge variability with soil type, each Thiessen polygon was intersected by the soil type shapefile using GIS to further divide each rainfall polygon to areas of different soil types that carry different fractions of recharge from rainfall. Thereafter, total recharge from rainfall (R_{ra}) was computed using the following equation (2):

$$R_{ra} = \sum_{x=1}^{y} (ra_x \times Ara_x \times fra_x) \quad (2)$$

where ra_x is the monthly rainfall depth for each subdivided polygon x (L/T); Ara_x is the area for each subdivided polygon (L^2); fra_x is the fraction of recharge for a specific soil type (dimensionless); and y is the total number of subdivided polygons (dimensionless). The estimation of the areas of the subdivided polygons (Ara_x) was determined using GIS. In general and in addition to the soil type, the value of fra_x depends on different factors such as surface slope, land cover class, and land use type. It should be mentioned that in populated areas (built-up areas), recharge can be set to zero under the assumption that the built-up areas are totally impervious.

2.1.3.2. Recharge from irrigation return-flow. Generally, not all the irrigation water is consumed by plants. In fact, a proportion of this may percolate beyond the soil zone and later recharges the aquifer. This recharge equals the multiplication of the total volume of water used for irrigation by the fraction of return-flow as in the following equation:

$$R_{Ir} = Q_{Irr} \times \delta_{Irr} \quad (3)$$

where Q_{Irr} is the total monthly volume of water used for irrigation in the study area (L^3/T) and δ_{Irr} is the fraction of irrigation return-flow that becomes recharge (dimensionless). In turn, Q_{Irr} can be computed using the following equation:

$$Q_{Irr} = \sum_{u=1}^{v} [d_{Irr\,u} \times A_u \times BIN_u(t)] \quad (4)$$

where d_{Irru} is the monthly irrigation rate for each crop type u (L/T); A_u is the area for each crop type (L^2); $BIN_u(t)$ is a binary multiplication factor to account for the months that may receive irrigation water where t is the month that represents the simulation time step; and v is the total number of crop types in the study area associated with the land cover type. The area of each land use type (crop type) was computed using GIS. Since there are months without irrigation, irrigation in these months was nullified. To do so, the monthly irrigation rate was multiplied by the binary factor (see $BIN_u(t)$ in equation (4)) where a value of 1 was used for the months when there was irrigation and 0 when otherwise. The multiplication of the area by the monthly irrigation rate gives the monthly irrigation volume for each land use type. The summation of all these monthly volumes across the different crop types produces the total volume of the recharge from irrigation return-flow.

2.1.3.3. Recharge from wastewater leakage. In this subsection, the quantification procedure of recharge from wastewater leakage from the sewerage system is illustrated. This recharge equals the multiplication of the total volume of wastewater leakage from the sewerage system by the fraction of the wastewater recharge as illustrated in the following equation:

$$R_{WWL} = WWL \times \delta_{WWL} \quad (5)$$

where WWL is the total monthly wastewater leakage from the sewerage network (L^3/T) and δ_{WWL} is the recharge fraction of wastewater leakage (dimensionless). The monthly wastewater leakage is calculated using the following equation:

$$WWL = POP \times W_{consm} \times \gamma \times \Omega_{ww} \times PERSERV \quad (6)$$

where POP is the total monthly population living within the study area (capita); W_{consm} is the per capita monthly water consumption (L^3/T/capita); γ is the fraction of water that becomes wastewater (dimensionless); Ω_{ww} is the leakage fraction of wastewater from sewerage system (dimensionless); and PERSERV is the fraction of population served by the sewerage system (dimensionless).

To find out the total volume of wastewater leakage from the sewerage system, the following issues were considered. Firstly, the population size in the study area served by the wastewater collection network was estimated on monthly basis. Secondly, the per capita water consumption was computed by considering the total monthly water consumption for the study area. Thirdly, the determination of the fraction of wastewater leakage was left to be determined through the calibration process since no estimates of high certainty were available for this parameter.

2.1.3.4. Recharge from water network leakage. This recharge component equals the multiplication of the total volume of water leakage from the distribution network and the fraction of the leakage that becomes recharge as can be seen from equations (7) and (8).

$$WL = PUMPDOM \times \Omega_w \quad (7)$$

where WL is the monthly volume of leakage from the water distribution network (L^3/T); PUMPDOM is the volume of water pumped for domestic purposes on monthly basis (L^3/T); and Ω_w is the water leakage fraction from the distribution network (dimensionless). The recharge to the aquifer from the leakage of water from the distribution network is given by the following formula:

$$R_{WL} = WL \times \delta_{WL} \quad (8)$$

where δ_{WL} is the fraction of water leakage that becomes recharge (dimensionless).

2.1.3.5. Recharge from cesspits. The recharge from cesspits equals the total wastewater leaching from cesspits multiplied by the fraction of wastewater that becomes recharge. Using a similar concept to that used in computing wastewater recharge, the total wastewater generated from cesspits was computed as shown in equations (9) and (10).

$$R_{CSPT} = WW_{cesspits} \times \delta_{CSPT} \quad (9)$$

and

$$WW_{cesspits} = POP \times W_{consm} \times \gamma \times (100 - PERSERV) \quad (10)$$

where $WW_{cesspits}$ is the total monthly wastewater generated from cesspits (L^3/T) and δ_{CSPT} is the recharge fraction of wastewater from cesspits (dimensionless). The use of equation (10) is under the assumption that the cesspits are not lined. In addition, δ_{CSPT} was assumed to remain constant over time though a time-based relationship may exist for this recharge fraction.

2.1.4. Lateral outflow

Lateral outflow (G_o) was computed using the same concept for determining lateral inflow. However, the fundamental difference between lateral inflow and outflow is that in the case of outflow, the water table elevation in the aquifer is higher than that of the specific segment adjacent to the model domain.

2.1.5. Water pumped for irrigation

Water pumped for irrigation (Q_{Irr}) was only considered for areas that receive irrigation water. It was estimated using equation (4).

2.1.6. Water pumped for domestic purposes

The water consumed for domestic purposes (Q_{DO}) equals the population size multiplied by the per capita monthly water consumption. To account for the actual amount being pumped from the aquifer, the following equation was used:

$$Q_{DO} = \frac{(POP \times W_{consm})}{(1 - \Omega_w)} \quad (11)$$

2.2. Development of the quality LPM

As depicted in Fig. 2, the quality LPM relies on the outcome of the quantity model, which represents the variability in the water table elevation with time; $h(t)$. A mass balance of nitrate for the model domain was employed in order to simulate the overall nitrate concentration.

The sources of nitrate which were considered in model development include lateral inflow, artificial recharge, fertilizer loading, and recharge. Denitrification, lateral outflow, and groundwater pumped for domestic and irrigation purposes were considered as the main sinks of nitrate from the GCJC area. Fig. 2 depicts the development of the conceptual quality LPM. It should be kept in mind that for nitrate sinks, there is no need to specify any concentration value since aquifer average concentration was employed.

One important issue to consider here is the nitrogen cycle in the unsaturated zone. Since an LPM is being developed with the intention of maintaining simplicity, linear coefficients were considered to account for the nitrogen cycle. In doing so, we follow the work of Mercado (1976) where he utilized two linear proportion coefficients. The idea from using these two coefficients is to assume that part of the applied nitrogen from the different sources will leach to groundwater while the rest will be lost or transformed in the soil zone and will not reach the aquifer. Cox and Kahle (1999) utilized linear coefficients to compute nitrate leaching to groundwater in Whatcom County, Washington, US. Despite the fact that a model for the nitrogen dynamics in both the saturated and unsaturated zones would be more accurate, this approach using the linear coefficients is simpler and more practical. Moreover, because the linear coefficients can be determined through the calibration process, the model would be accurate enough.

The following sections illustrate the elements pertaining to the development of the quality LPM.

2.2.1. Nitrate from lateral inflow

The monthly amount of nitrate (as mass) that enters the aquifer with lateral inflow from the surrounding areas (NO_3G_{in}) can be calculated using the following equation:

$$NO_3G_{in} = \sum_{j=1}^{z} (G_{in\,j} \times C_{in\,j}) \quad (12)$$

where NO_3G_{in} is the mass of nitrate that enters the study area by lateral inflow (M/T) and C_{inj} is the average concentration of nitrate for segment j (M/L^3).

Using GIS, maps of average nitrate concentrations for the study area can be created using the following procedure: (i) the locations of nitrate sampling wells can be specified using a GIS shapefile; (ii) the average nitrate concentration for each well is computed; (iii) after that, Thiessen polygons are created for each well such that each transpired polygon is represented by a single well and thus a single nitrate concentration value; and (iv) the segments of the model domain are intersected by these concentrations. This enables the designation of nitrate concentration for lateral inflow that enters the study area through each segment. These concentrations are multiplied by their corresponding lateral inflow volumes to obtain nitrate mass flux. Summing up these mass fluxes provide the amount of nitrate that enters the model domain by lateral inflow as shown in equation (12).

2.2.2. Nitrate from artificial recharge

The monthly amount of nitrate (as mass) that enters the aquifer through artificial recharge (NO_3Q_A) can be calculated using the following equation:

$$NO_3Q_A = Q_{Ar} \times C_{Ar} \quad (13)$$

where C_{Ar} is the nitrate concentration in artificial recharge for a specific month (M/L^3).

2.2.3. Nitrate from fertilizer surplus

The monthly amount of nitrate (as mass) that enters the aquifer due to the fertilizer use in agricultural areas (NO_3SURP) can be calculated using the following equations:

$$NO_3SURP = SURP \times \alpha_{FERT} \quad (14)$$

$$SURP = \sum_{u=1}^{v} [(FERT_u - CONS_u) \times A_u \times BIN_u(t)] \quad (15)$$

$$CONS_u = FERT_u \times PERCONS \quad (16)$$

where SURP is the total monthly mass of fertilizer surplus from all the agricultural land use classes and the corresponding crops (M/T); α_{FERT} is a fraction for fertilizers that describes the transformations related to nitrogen in the unsaturated zone (dimensionless); FERT$_u$ is the amount of fertilizer applied for each type of land use per unit area (M/L^2/T); CONS$_u$ is the consumption of fertilizer for each crop per unit area (M/L^2/T); and PERCONS is the fraction of applied fertilizers that would be taken up by plants.

To implement equations (14)–(16), many parameters must be determined. First of all, the amount of fertilizers being applied to different crop types should be determined. The area of each crop type can be determined using GIS. An assumption was made that not all the fertilizers are taken up by plants and that just a percentage of fertilizers is consumed. This leaves an amount that is ready to leach to groundwater. The equations in (14)–(16) are utilized for each crop type and the summation gives the total surplus of NO_3 from fertilizers.

2.2.4. Nitrate from recharge

Total nitrate that reaches the aquifer via recharge equals the summation of nitrate that comes from rainfall, irrigation return-flow, wastewater leakage, leakage from water distribution networks, and cesspits. This can be expressed by the following equation:

$$NO_3R = NO_3R_{ra} + NO_3R_{Ir} + NO_3R_{WWL} + NO_3R_{WL} + NO_3CSPT \quad (17)$$

where NO_3R is the total monthly mass of nitrate that enters the aquifer via recharge (M/T); NO_3R_{ra} is the monthly mass of nitrate that enters the aquifer via recharge from rainfall (M/T); NO_3R_{Ir} is the monthly mass of nitrate that enters the aquifer via irrigation return-flow (M/T); NO_3R_{WWL} is the monthly mass of nitrate that enters the aquifer via leakage of wastewater (M/T); NO_3R_{WL} is the monthly mass of nitrate that enters the aquifer via leakage from the water distribution network (M/T); and NO_3CSPT is the monthly mass of nitrate that enters the aquifer from cesspits (M/T). In the following subsections, a detailed illustration of all the elements that appear in equation (17) is provided.

2.2.4.1. Nitrate from rainfall recharge. Nitrate that enters the aquifer from rainfall recharge can be estimated using the following equation:

$$NO_3R_{ra} = R_{ra} \times C_{ra} \times \alpha_{ra} \quad (18)$$

where C_{ra} is the monthly nitrate concentration in rainfall (M/L^3) and α_{ra} is the fraction for rainfall that describes the transformations in the soil zone (dimensionless).

2.2.4.2. Nitrate from irrigation return-flow recharge. Nitrate that enters the aquifer from irrigation return-flow can be estimated using the following equation:

$$NO_3R_{Ir} = R_{Ir} \times C_{Ir} \times \alpha_{Ir} \quad (19)$$

where C_{Ir} is the monthly nitrate concentration in irrigation return-flow (M/L^3) and α_{Ir} is a fraction for irrigation that describes the transformations in the soil zone (dimensionless).

The value of C_{Ir} equals the initial nitrate concentration, which is C_o for the entire aquifer for the first time step (at the beginning of simulation). Thereafter, for each time step (each month), nitrate concentration at the preceding time step is used. The value of recharge from irrigation return-flow is obtained from equation (3).

2.2.4.3. Nitrate from leakage of wastewater. Nitrate that enters the aquifer from leakage of wastewater can be estimated using the following equation:

$$NO_3R_{WWL} = R_{WWL} \times C_{WWL} \times \beta_{WWL} \tag{20}$$

where C_{WWL} is the total nitrogen concentration in the leakage of wastewater (M/L^3) and β_{WWL} is a fraction for wastewater leakage that describes the transformations in the soil zone (dimensionless). The value of recharge from leakage of wastewater is obtained from equation (5).

2.2.4.4. Nitrate from leakage of water. Nitrate that enters the aquifer from leakage of water can be estimated using the following equation:

$$NO_3R_{WL} = R_{WL} \times C_{WL} \times \alpha_{WL} \tag{21}$$

where C_{WL} is the nitrate concentration in the leaking water (M/L^3) and α_{WL} is a fraction of water leakage that describes the transformations in the soil zone (dimensionless). The value of recharge from leakage of water is obtained from equation (8). C_{WL} was assumed equal to the nitrate concentration of the groundwater of the GCJC as computed by the model.

2.2.4.5. Nitrate from cesspits. Nitrate that enters the aquifer from cesspits can be estimated using the following set of equations:

$$NO_3R_{CSPT} = NO_3GEN_{CSPT} \times \beta_{CSPT} \tag{22}$$

$$NO_3GEN_{CSPT} = NGEN_{CSPT} \times FraNO_3N \tag{23}$$

$$NGEN_{CSPT} = POP \times N_{CAPITA} \times (100 - PERSERV) \tag{24}$$

where NO_3GEN_{CSPT} is the nitrate mass that originates in cesspits (M/T); β_{CSPT} is a fraction for cesspits that describes the transformations in the soil zone (dimensionless); $NGEN_{CSPT}$ is the total mass of nitrogen generated from the cesspits of the study area (M/T); $FraNO_3N$ is the fraction of nitrogen from cesspits that becomes nitrate (dimensionless); and N_{CAPITA} is the generated mass of nitrogen per capita (M/T).

2.2.5. Nitrate lost through lateral outflow

The amount of nitrate mass that leaves the aquifer through lateral outflow (NO_3G_o) from all the segments is computed using the following equation:

$$NO_3G_o = C\sum_{j=1}^{z} G_oj \tag{25}$$

where C is the average nitrate concentration in the aquifer (M/L^3) and Z is the total number of segments. Equation (25) is employed for each segment j by summing up the lateral outflow and multiplying this by the average nitrate concentration in the aquifer.

2.2.6. Nitrate lost through irrigation

The amount of nitrate lost from the aquifer through water pumped for irrigation (NO_{3Irr}) is computed by the following equation:

$$NO_{3Irr} = Q_{Irr} \times C \tag{26}$$

2.2.7. Nitrate lost through domestic use of groundwater

The amount of nitrate lost from the aquifer through water pumped for domestic purposes (NO_{3DO}) is given by the following equation:

$$NO_{3DO} = Q_{DO} \times C \tag{27}$$

2.2.8. Nitrate lost through denitrification

The amount of nitrate lost due to denitrification. (NO_{3DEN}) is given by equations (28) and (29):

$$NO_{3DEN} = V_{w0} \times \lambda \times C \tag{28}$$

$$V_{w0} = \left(h_0 + |D_p|\right) \times A \times \Phi \tag{29}$$

where V_{w0} is the monthly water volume in the aquifer at the beginning of each time step (L^3); λ is the first order decay coefficient of the denitrification reaction (T^{-1}); h_0 is the water table elevation with reference to sea level at the beginning of each time step (L); A is the total area of the model domain (L^2); and Φ is the aquifer average effective porosity (dimensionless). The decay coefficient of nitrate (λ) is given by the following equation (Shamrukh et al., 2001):

$$\lambda = \frac{0.693}{t_n} \tag{30}$$

where t_n is the half-life of nitrate (T). In general, a nitrate half-life time of 2.3 years can be used (Frind et al., 1990).

2.3. Development of the mathematical models

As mentioned earlier, the development of the LPM for nitrate concentration in groundwater requires the development of a model for simulating the water table elevation. Two major equations, (31) and (32) are used to implement the mass balance approach considering that the aquifer is simulated as a single cell. The general mass balance equation for groundwater quantity and quality can be expressed by the following two equations:

$$\sum Q_{IN} - \sum Q_{OUT} = \Delta S_W \tag{31}$$

$$\sum [Q_{IN} \times C_{IN}] - C \times \sum Q_{OUT} = \Delta S_N \tag{32}$$

where Q_{IN} is the amount of water that enters the model domain from a specific source (L^3/T); ΣQ_{OUT} is the total amount of water that leaves the model domain from all the sources (L^3/T); ΔS_W is the change in the water storage in the aquifer of the study area for each time step (L^3/T); C_{IN} is the average concentration of nitrate for a specific water source Q_{IN} (M/L^3); C is the average nitrate concentration in the aquifer (M/L^3); and ΔS_N is the change in the mass of nitrate in the aquifer of the study area for each time step (M/T). For the groundwater quantity (the water table elevation), equation (31) becomes:

$$G_{in} + Q_{Ar} + R_{ra} + R_{Ir} + R_{WWL} + R_{WL} + R_{CSPT} - G_o - Q_{Irr} - Q_{DO} = \Delta S_W \tag{33}$$

$$V_{w1} = \Delta S_W + V_{w0} \tag{34}$$

$$h_1 = \frac{V_{w1}}{(A \times \Phi)} + D_p \tag{35}$$

where V_{w1} (L^3/T) is the water volume at the end of each time step (when the water table elevation equals h_1). For the groundwater quality (the nitrate concentration in the aquifer), equation (31) becomes:

$$[NO_3G_{in} + NO_3Q_A + NO_3SURP + NO_3R_{ra} + NO_3R_{Ir} + NO_3R_{WWL} + NO_3R_{WL} + NO_3R_{CSPT}][NO_3G_o + NO_{3Irr} + NO_{3DO} + NO_{3DEN}] = \Delta S_N \quad (36)$$

$$\Delta S_N = V_{w1}C_1 - V_{w0}C_0 \quad (37)$$

$$C_1 = \frac{\Delta S_N + V_{w0}C_0}{V_{w1}} \quad (38)$$

where C_0 is the average nitrate concentration (M/L^3) at the beginning of each time step and C_1 is the average nitrate concentration at the end of each time step (M/L^3). In the first time step, C_0 equals the initial concentration in the aquifer. The solution of equation (35) using equations (33) and (34) provides the variability of water table elevation with time. This enables the computation of the variability of the water volume in the aquifer and thus enables the simulation of the nitrate concentration in the aquifer as shown in Fig. 2. The solution of equation (38) using equations (36) and (34) provides the overall variability of nitrate concentration in the aquifer with time.

2.4. Numerical solution of the LPMs

The last step in the model development is to obtain a numerical solution. The numerical solutions of equations (35) and (38), to find out $h(t)$ and $C(t)$, respectively, can be obtained using a spreadsheet such as MS Excel or through developing a code based on any programming language.

3. Model application

The LPMs were implemented in the GCJC area located in the north of Gaza Strip, Palestine (see Fig. 1). The following subsections provide a description of the study area along with an illustration of the development of the mathematical models.

3.1. Description of the study area

GCJC area is located in the north of Gaza Strip. Gaza Strip is a narrow and low-lying stretch of sand dunes along the eastern Mediterranean Sea. The total area of GCJC area is 58 km^2 with almost a half million persons. The GCJC area was chosen as a study area for several reasons. These include the large density of population; the on-going contamination by nitrate in the study area; and the high number of municipal wells (39 wells) that operate in the GCJC area for water supply. In addition, the nitrate contamination problem is attributed to internal and external contamination sources and this makes it an interesting case to consider.

In the GCJC area; peak months of rainfall are December and January. The total annual rainfall for the year 2003–2004 ranges between 340 mm up to 500 mm based on the data obtained from the Palestinian Water Authority (PWA). Evaporation is high in summer where there is always a water deficit. The breakdown of land use by category is summarized in Table 1. Agricultural land occupies about 34% of the land surface. Built-up areas (residential locations) occupy 45% while almost 21% of the land is characterized as open area (undeveloped natural lands).

The coastal aquifer of the Gaza Strip consists of the Pleistocene age Kurkar Group and recent (Holocene age) sand dunes. The Kurkar Group consists of marine and aeolian calcareous sandstone (kurkar), reddish silty sandstone (hamra), silts, clays, unconsolidated sands, and conglomerates. Clay formations are present along the coast at various depths. They pinch out about 5 km from present coastline and appear to become more important towards the base of the Kurkar Group.

Table 1
Detailed categories of land use classes for the GCJC area. This table is based on the land use map of the entire Gaza Strip as obtained from the PWA and later geo-processed using GIS for the GCJC area.

Land use category	Area (km^2)	%
Built-up	26.27	45
Citrus	5.24	9
Dates	2.60	4
Field crops	6.42	11
Fruits	2.86	5
Grapes	1.26	2
Greenhouses	0.51	1
Horticulture	1.08	2
Olives	0.09	0
Open area	12.22	21

There are more than 500 licensed wells within the GCJC area. The majority of these wells are privately owned and used for agricultural purposes. A total of 39 wells are owned and operated by municipalities and are used for domestic water supply. Most agricultural wells in GCJC are shallow. Municipal wells are deeper depending on location and distance from the coast. Water table contours in meters above mean sea level for the study area are depicted in Fig. 3 for the year 2000 along with the direction of groundwater flow. For additional information related specifically to the soil and geology of the study area, the reader can refer to Metcalf and Eddy (2000), Baalousha (2003), Qahman (2004), and Shomar et al. (2005).

3.2. Nitrate pollution in the groundwater of GCJC area

There are many sources of contamination in Gaza Strip and the study area where the groundwater of GCJC area is highly vulnerable to pollution (Al-Agha, 1997; Shomar, 2006; Agha, 2006). Many years of over-pumping have resulted in seawater intrusion and upconing of saline groundwater. Furthermore, human activities including agriculture and inadequate wastewater disposal have increased groundwater contamination levels. Intensive cultivation and efforts to boost production have led to excessive use of fertilizers, pesticides, herbicides and soil fumigants, while collection, treatment and disposal of wastewater and solid waste (including hazardous materials) are inadequate in many areas in GCJC and Gaza Strip as well (UNEP, 2003).

Fig. 4 depicts the spatial distribution of average nitrate concentration for the years 2003 and 2004 based on the nitrate data obtained from the PWA. Fig. 4 was obtained by interpolating the point observations of nitrate for the years 2003 and 2004. Interpolation was accomplished using the inverse distance weighting method with the aid of GIS.

3.3. Development of the numerical LPMs for GCJC area

In order to compute the lateral inflow that enters the study area, the boundaries were discretized into segments as mentioned earlier and shown in Fig. 3. Total lateral inflow equals the summation of all lateral inflows through all segments designated in Fig. 3. The hydraulic conductivity was assumed to be constant for the GCJC area since the developed model is a lumped-parameter model. Hydraulic conductivity values for GCA have been reported to be in the range of 20–80 m/d (Metcalf and Eddy, 2000).

To find the hydraulic gradient and the cross-sectional area of the flow, a water table contour map was created using GIS. This map

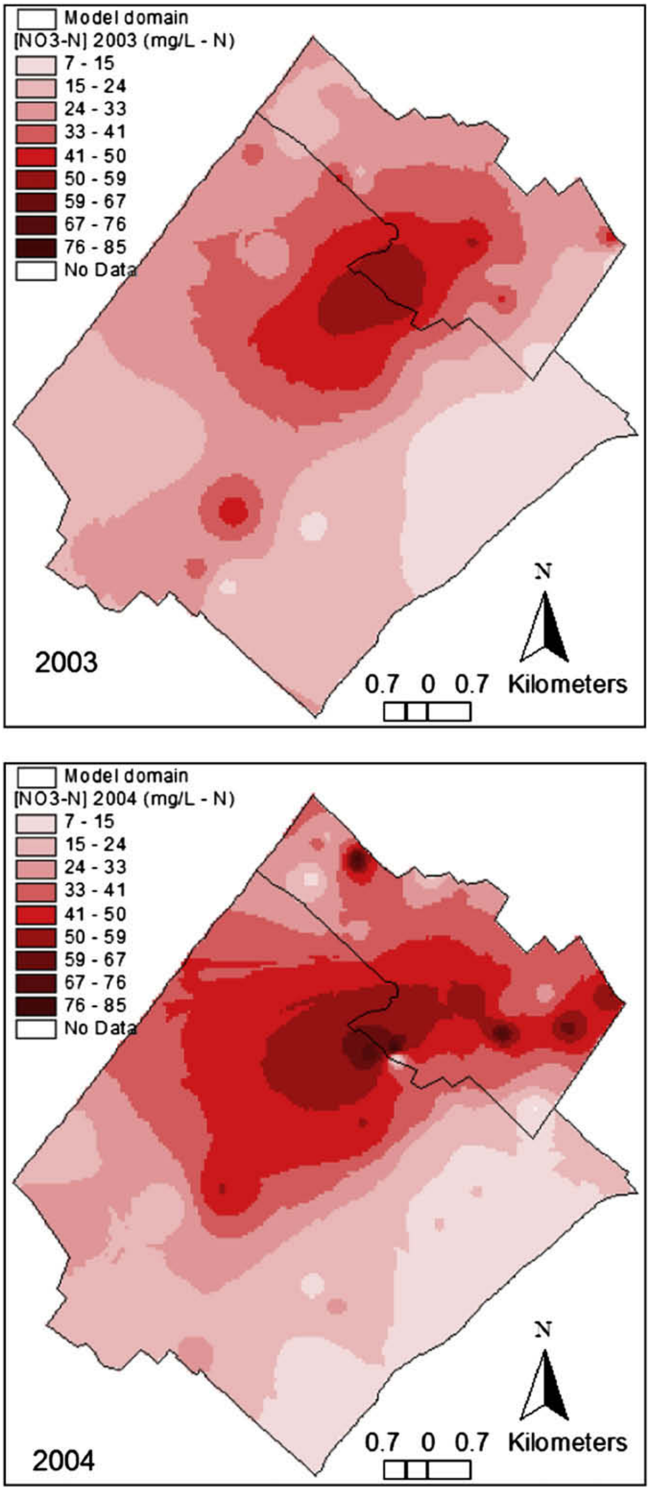

Fig. 4. Nitrate concentration distribution in mg/L (NO_3-N) in the GCJC area for the years 2003 and 2004.

was obtained from a groundwater flow model for the entire Gaza Strip after clipping it to fit the GCJC area. In this map, the difference between any two consecutive contour lines is always constant which results in a constant change in the hydraulic head (Δh) between any two contour lines. Thus, the changes in the distances between the contour lines dictate the values of the gradient and dictate the segmentation of the boundaries of the model domain. The saturated thickness was assumed to decrease on monthly basis based on the average decline in the water table that was observed for the period from 1970 to 2000 which equals a total of 3 m (Qahman, 2004). To find the saturated thickness, the distance from sea level to the water table (WT) and the distance from sea level to the bottom of the aquifer (D_p) were used as described earlier.

In the study area, there are no injection wells. As such, Q_{Ar} was set to zero. The fraction of return-flow from irrigation was set to 15%, which is within the range of 15–30% (Metcalf and Eddy, 2000). The area of each land use type (crop type) was obtained using GIS. Based on the personal communications, the monthly irrigation rates for each crop type were obtained (Dr. Hassan Abu Qaoud, personal communication, College of Agriculture, An-Najah National University, Nablus, Palestine, 2005). Since there are months without irrigation, irrigation rates in these months were nullified.

The initial population in the study area in 1997 was found to be 473,383 persons. Ninety percent of the population is served by the sewerage system (Dr. Said Ghabayen, personal communication, College of Engineering, University of Palestine, Gaza, Palestine, 2005). As such, the percentage of the population of GCJC area that uses cesspits is 10%. Using a growth rate of 3.5%, the monthly population was estimated. The percentage of wastewater leakage from the sewerage network was determined through the calibration process. The percentage of water that becomes wastewater was taken as 80% (PWA, 2006).

4. Results and analysis

4.1. Model calibration

Model calibration was carried out in two stages. In the first stage, the quantity LPM was calibrated. The calibration process was carried out by forcing the model to produce a decline rate in water table elevation similar to the reported rates in the literature (Qahman, 2004). In doing so, the "Goal Seek" option of MS Excel was used to determine the appropriate hydraulic conductivity value after trying different values of wastewater leakage percentage. The calibrated average hydraulic conductivity value for the GCJC area is 42.1 m/d and wastewater leakage percentage is 20%. The calibration covers the period from 2000 to 2003 with monthly time steps.

In the second stage, the quality LPM was calibrated. Optimization was utilized herein in model calibration using the "Solver package" of MS Excel. The "Solver package" has three main components and these are: (i) *the objective function*: in our case, the objective function is to minimize the summation of square errors that represent the differences between the observed values of the average nitrate concentrations for years 2000–2003 and the simulated values; (ii) *the decision variables*: these decision variables are the calibration parameters and include the following: (a) lateral inflow; (b) fertilizer application rate; (c) the α fractions for rainfall, irrigation, water leakage, and fertilizers; and (d) the β fractions for wastewater leakage and cesspits; (iii) *the constraints*: these represent realistic ranges of the calibration parameters.

According to Mercado (1976), the ranges for the fractions α and β were from 27% to 46% and from 70% to 100%, respectively. Lateral inflow and the fertilizer application rate were calibrated by considering a multiplication factor for each and the calibration process becomes the determination of these factors. Calibration results of the quality LPM are depicted in Fig. 5. The simulated nitrate concentrations for the years 2000, 2002, and 2003 closely match the observed values. For year 2001, it is apparent that there is a higher error compared to the other three years. Nevertheless, the difference between the observed and simulated nitrate concentrations for year 2001 is less than 15%, which is acceptable.

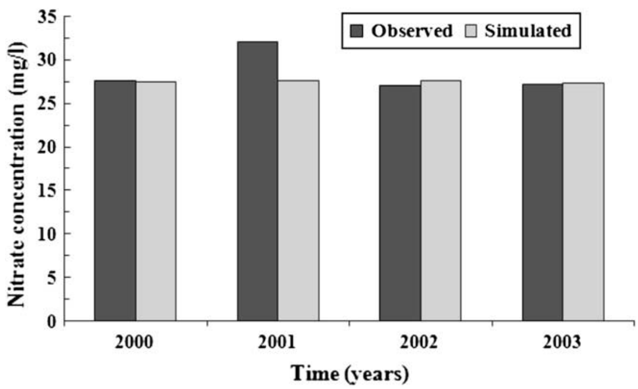

Fig. 5. The average nitrate concentration for the observed and simulated values for years 2000–2003.

4.2. Sensitivity analysis

A set of parameters were selected for the sensitivity analysis and these are summarized in Table 2. The values of the parameters summarized in Table 2 were perturbed by 10% and the corresponding head and concentration values were simulated using the calibrated LPMs. Thereafter, the relative sensitivity coefficients ($\upsilon_{\mathcal{R}}$) for head and nitrate concentration were computed using the following formula:

$$\upsilon_{\mathcal{R}} = \frac{\Delta M_O/M_O}{\Delta M_I/M_I} \quad (39)$$

where M_O is the model output; M_I is the model input; and ΔM_O and ΔM_I are the changes in model output and input parameter values, respectively. $\upsilon_{\mathcal{R}}$ is convenient for comparing sensitivity coefficients for different parameters of different physical units.

Fig. 6 shows the relative sensitivity coefficients of the water table elevations for the parameters summarized in Table 2. With decreases in the selected parameters, different responses in terms of corresponding increase and decrease in water table elevation values are encountered. Obviously, parameter 18 (water consumption) had the highest value and thus has the highest impact on water table elevation. Parameters 1, 2, 6, 16, 18, 19, 22, and 23 (see Table 2 for parameter description) have sensitivity coefficients that are notably high.

Fig. 7 shows the different relative sensitivity coefficients of nitrate concentration in the aquifer for the selected model input parameters summarized in Table 2. Parameter 12 (initial nitrate concentration) has the highest positive value of the sensitivity coefficient while parameter 23 (percentage of area serviced by the sewerage system) had the highest negative sensitivity coefficient. The model output in terms of nitrate concentration is insensitive to the initial water table elevation and thus has a zero sensitivity coefficient.

Upon comparing both Figs. 6 and 7, we notice that parameters 6, 22, and 23 have a large impact on the output of the developed LPMs in terms of water table elevation and nitrate concentration. On the contrary, the parameters 3, 7, 8, 13, 14, and 17 are of low impact on nitrate concentration.

Table 2
Selected parameters for the sensitivity analysis of the LPMs.

#	Parameter
1	Hydraulic conductivity
2	Percentage of wastewater generation from water
3	Growth rate
4	Fractions (rainfall, artificial recharge, water leakage, and fertilizers)
5	Fractions (wastewater leakage and cesspits)
6	Recharge fraction for sandy soil (regosols)
7	Recharge fraction for dark-brown soil
8	Recharge fraction for sandy soil (loess soil)
9	Leakage percentage from the water distribution network
10	Leakage percentage of sewerage system
11	Per capita monthly generation rate of nitrogen
12	Initial nitrate concentration
13	Initial water table elevation
14	Fraction of irrigation return-flow
15	Fraction of wastewater that becomes recharge
16	Fraction of water recharge
17	Fraction of cesspits recharge
18	Water consumption
19	Irrigation rate
20	Concentration of nitrate that enters the study area via lateral inflow
21	Fertilizer application rate
22	Rainfall depth
23	Coverage percentage by the sewerage system

4.3. Analysis and discussion of model output

Water table elevation is the main output from the quantity LPM. The water table elevation for the groundwater of the study area shows a variation where the maximum value occurs in March while the minimum value occurs in November. This behavior is definitely attributed to the decrease in recharge from rainfall and the increase in the water consumption (withdrawal) during the summer time. To illustrate the issue of the declining head over time, Fig. 8 was developed. The figure depicts the variability of water table elevation and the difference between the total monthly input and output of groundwater for the GCJC study area which represents the monthly change in groundwater storage. Apparently, more groundwater leaves the GCJC area than what enters it. This situation creates a deficit in groundwater storage in GCJC area over time. The analysis of the water budget for the groundwater of the GCJC area for year 2003 shows that recharge from rainfall has the maximum contribution of water where it accounts for 31% of the incoming quantity followed by the leakage from the water distribution network (28%) and lateral inflow (25%). The remainder (16%) comes from cesspits, irrigation return-flow, and wastewater leakage. As for groundwater outflow, water pumped for domestic purposes accounts for 70% of water leaving the GCJC area while water pumped for agricultural irrigation accounts for 29% from the total and the remainder is for lateral outflow.

Fig. 9 depicts the time series of the simulated average nitrate concentration for the groundwater of the GCJC area for the period from October of 1999 to April of 2004. The nitrate concentration ranges between 26.5 mg/L NO_3-N and 28.5 mg/L NO_3-N. The maximum value of nitrate concentration occurs in November when the average water table is at its minimum value. Obviously, all the monthly values of nitrate concentrations as simulated by the LPM exceed the MCL of 10 mg/L NO_3-N.

The nitrate budget for the groundwater of the GCJC area shows that 30% of the incoming nitrate is attributed to the lateral inflow. This brings in the highest amount of nitrate compared to the other sources. Hence, the adjacent neighboring areas must be in our management consideration. The amount of nitrate from cesspits (15%) is less than that from wastewater leakage (24%). The contribution of fertilizers (15%) to overall nitrate input is less than that from wastewater leakage since we have a large residential area (the built-up area in the GCJC comprises about 45% of the total area). The remainder of nitrate input comes from rainfall recharge, irrigation return-flow, and water leakage from the distribution network.

Almost all the nitrate that is lost from the area is attributed to water pumping for domestic and agricultural purposes.

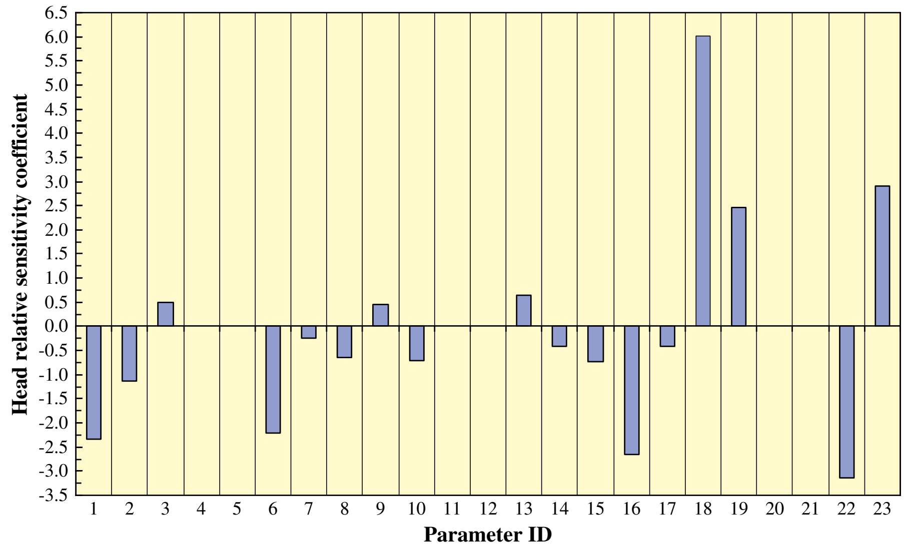

Fig. 6. Relative sensitivity coefficients of water table elevation for the parameters summarized in Table 2.

5. Management of nitrate contamination of the groundwater of GCJC area

In order to demonstrate the usefulness and applicability of the developed LPMs, the effectiveness of the different management options that aim at reducing nitrate concentration in the groundwater of GCJC area was assessed. Since the objective is to reduce nitrate concentration to the MCL, a management period was proposed such that the MCL would be met by the year 2015.

5.1. Proposed management options

In determining the related management options that address the nitrate contamination problem, a number of options were proposed and examined. The management options considered herein are: (i) reduction of nitrate concentration in lateral inflow (option 1); (ii) rehabilitation of the wastewater collection network (option 2); (iii) reduction in cesspit usage (option 3); (iv) restriction on the use of fertilizers (option 4); and (v) combining different management options from the abovementioned four options.

The choice of the abovementioned management options is based on the following considerations: (i) recommended for reducing nitrate concentration as indicated in previous studies (see for instance Hasler, 1998; McLay et al., 2001; Meisinger and Delgado, 2002; Kraft and Stites, 2003; Oenema et al., 2004; Almasri and Kaluarachchi, 2004a, 2004b; Matthies et al., 2006); (ii) they target nitrogen sources that are large contributors to the elevated nitrate concentration in the groundwater of GCJC area; and (iii) a consensus among the Palestinian stakeholders, decision makers, water resources experts, and environmentalists that the proposed management options address the major sources of nitrate contamination of the groundwater of Gaza Strip which includes the

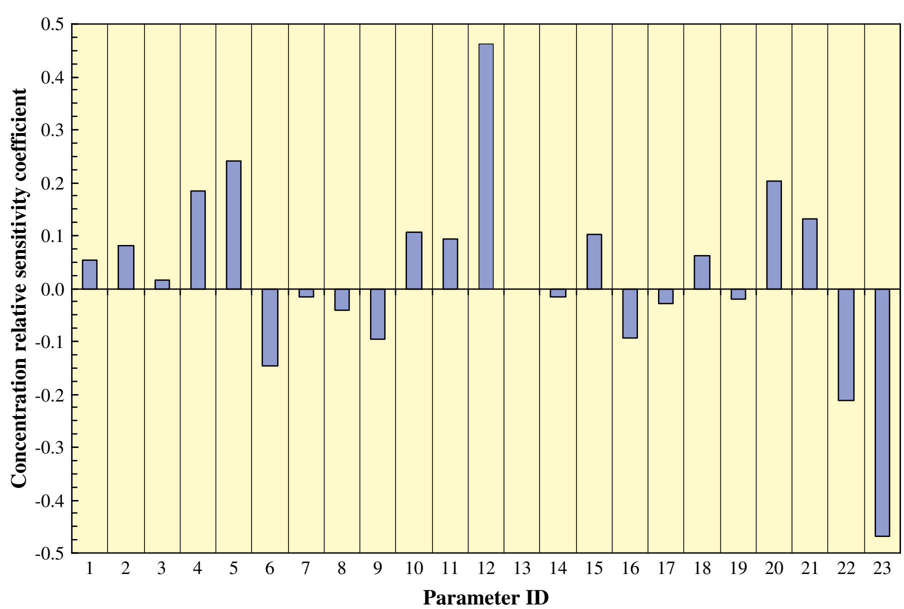

Fig. 7. Relative sensitivity coefficients of nitrate concentration for the parameters summarized in Table 2.

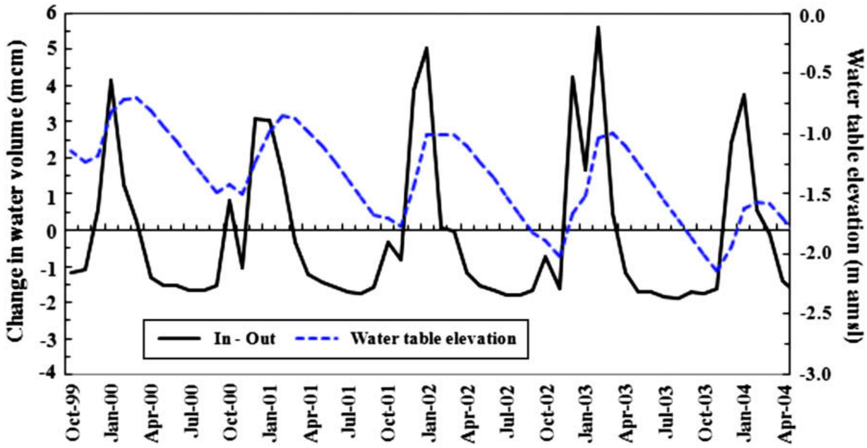

Fig. 8. Time series of the monthly difference between total input and output of groundwater volume for the GCJC area along with the groundwater table elevation.

GCJC area. However, it should be kept in mind that these options are generic and a field work and on-ground investigations should be carried out before implementation to figure out the rate of acceptance by the different stakeholders and the economic and social consequences (Turpin et al., 2005; Henriksen et al., 2007).

As indicated by Farmani et al. (2009), management of groundwater contamination is a complex interaction of different criteria (for instance economic, social, and ecological). In the following subsections, the impact of the abovementioned management options on nitrate concentration in the groundwater of the GCJC area is simulated and demonstrated using the developed LPMs. The analysis is limited to the determination of nitrate concentration and did not consider the economic ramifications since this is beyond the scope of the current work.

5.1.1. Option 1: reduction of nitrate concentration in lateral inflow

Lateral inflow to the groundwater of the GCJC area comes from the surrounding areas and carries with it nitrate to the GCJC area. This option implies the control on the use of nitrogen-based fertilizers in the surrounding agricultural areas and a reduction in nitrogen loading from the contributing sources. In this way, the nitrate concentration in the lateral inflow will be reduced as a result. To investigate the impact of the reduction of nitrate concentration in lateral inflow, a multiplication factor was considered in the quality LPM that influences the nitrate concentration value in the lateral inflow. This factor was then reduced in 10% increments up to 90%. Model simulated results are shown in Fig. 10.

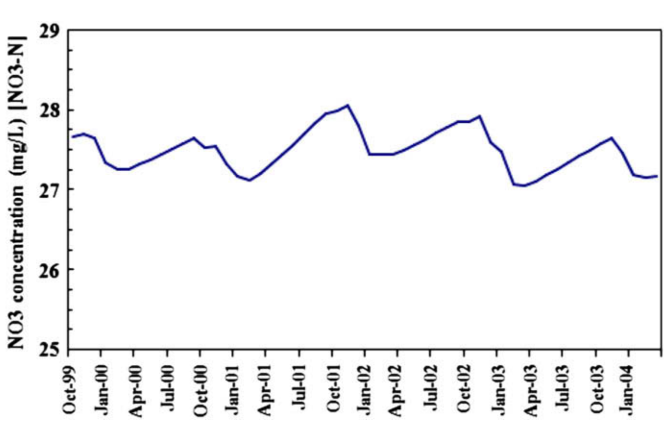

Fig. 9. The variability of the average nitrate concentration with time.

Even with extreme reductions in nitrate concentrations in lateral inflow, the overall concentration of nitrate for the GCJC area by the end of the management period is still greater than 23 mg/L.

5.1.2. Option 2: rehabilitation of the wastewater network

This management option involves a decrease in leakage rates from the sewerage system. In reality, this option entails the rehabilitation of the existing wastewater collection system. In model calibration, the leakage from the wastewater collection network was found to be 20%. Two leakage reductions of 50% and 100% were considered where 100% reduction in leakage represents a full rehabilitation of the wastewater collection network. Model simulated results are shown in Fig. 10. Under the option of no leakage from the wastewater network, the nitrate concentration is still greater than 24 mg/L.

5.1.3. Option 3: reduction in cesspit usage

The third management option is to have a full coverage of the sewerage system. This practice will transpire when the study area is being serviced entirely by the sewerage system and therefore there would be no cesspits at all. In the GCJC area, only 10% of the people use cesspits. Reduction percentages in the cesspit use were set to 50% and 100% where 100% reduction in the cesspit use implies a full coverage of the wastewater collection network for the GCJC area. Results are shown in Fig. 10. Even with the absence of cesspits in the study area, the nitrate concentration is still greater than 26 mg/L.

5.1.4. Option 4: restriction on the use of fertilizers

The last management option under consideration involves the restriction on the use of agricultural fertilizers in the GCJC area. Many studies demonstrated the importance of the application of fertilizers at rates that do not exceed the optimal crop demand (Yadav and Wall, 1998). To investigate the impact of fertilizer application, a range of 10–90% reduction in the fertilizer application rate was considered and results are depicted in Fig. 10. Even with restriction on the use of fertilizers, the nitrate concentration is still greater than 24 mg/L.

5.1.5. Combination of management options

Obviously, none of the past four single management options was individually able to reduce nitrate concentration below the MCL. In order to improve the efficiency of the management options in reducing nitrate contamination in the groundwater of GCJC area, a combination scheme of the management options was developed. Eleven combined management options were developed and their

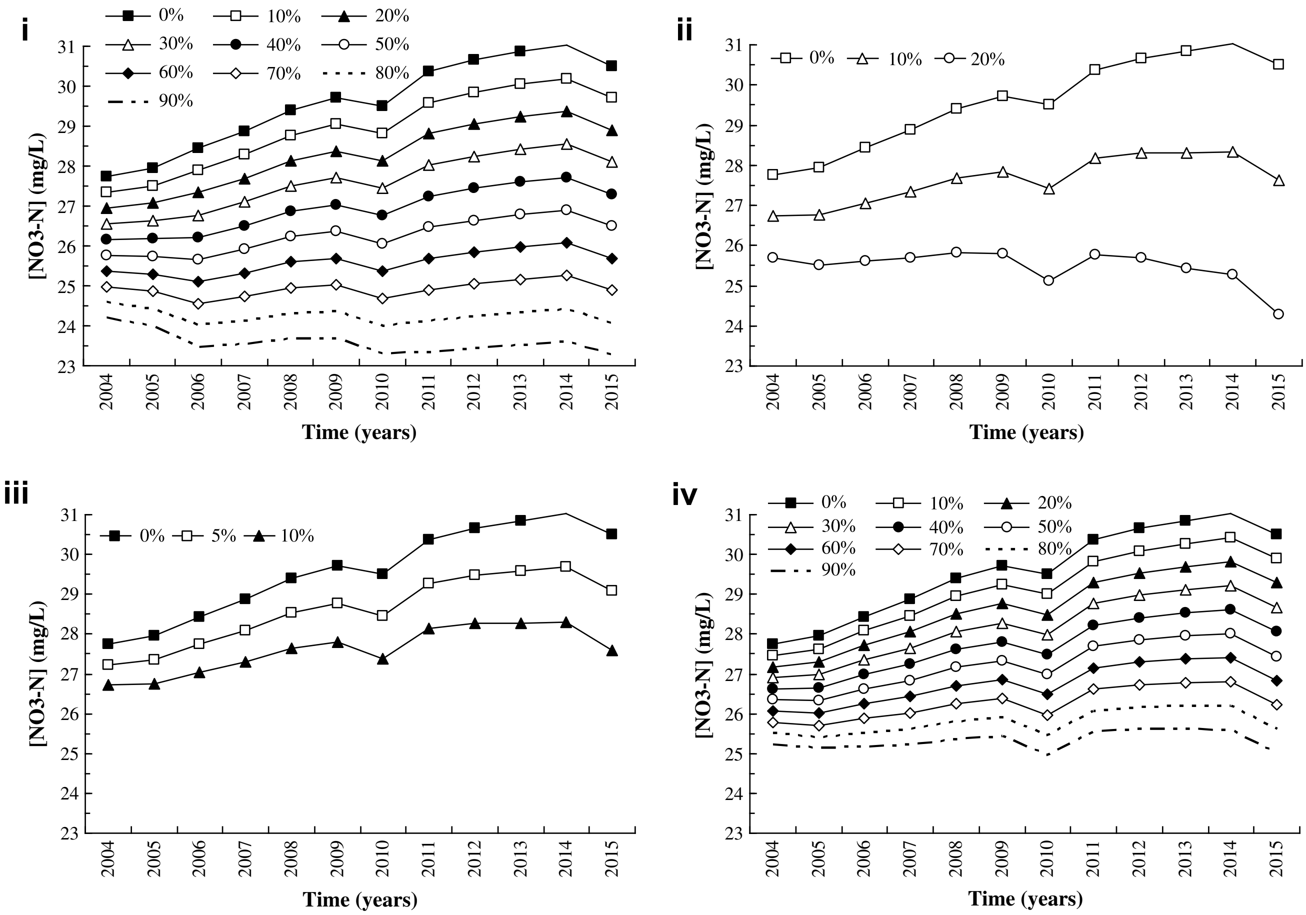

Fig. 10. The maximum nitrate concentrations in each year with different reduction percentages corresponding to (i) lateral inflow; (ii) leakage from the wastewater collection network; (iii) cesspits; and (iv) fertilizers.

effectiveness in meeting the MCL constraint was investigated. Three groups of combined management options were considered. The first group is comprised of six combined management options where each option consists of two different single management options as follows: $1+2$, $1+3$, $1+4$, $2+3$, $2+4$, and $3+4$ where numbers correspond to the single management option number as indicated earlier. The second group is comprised of four combined management options where each option consists of three different single management options as follows: $1+2+3$, $1+2+4$, $1+3+4$, and $2+3+4$. The third group is comprised of one management option that consists of the combined four single management options.

A range of 10–90% reduction in nitrate concentration for the option 1 and option 4 was considered. For option 2, two reduction percentages of 50% and 100% were considered for wastewater leakage from the collection network (a rehabilitation option) while for option 3 only 100% reduction was considered in the usage of cesspits (full coverage of the wastewater collection system). Based on the combinations of the management options and the different permutations in the reduction percentages, a total of 103 management scenarios were obtained. For these different scenarios, the efficiency in reducing nitrate concentration in the groundwater of GCJC area was assessed using the developed LPMs.

5.2. Analysis of the management options

As shown in Fig. 10, the simulation of each of the single management options suggests that the nitrate MCL level will not be achieved by the end of the management period. At the end of the management period, the single management option 1 yields a nitrate concentration of 23.3 mg/l, which yields the lowest nitrate concentration among the other three single management options. Management options 2, 3, and 4 yield nitrate concentrations of 24.3 mg/l, 27.6 mg/l, and 25.6 mg/l, respectively. That is, management option 1 is the most efficient among the four single management options. Since, none of these four options was able to meet the MCL constraint; combinations of the individual options were evaluated as illustrated earlier.

For the combined management options, there are only five scenarios that yield concentrations below the MCL. The first management scenario corresponds to the combined management options $1+2+4$ where this scenario implies a 90% reduction in nitrate concentration in lateral inflow; a full rehabilitation of the wastewater collection system, and a 90% reduction in the use of nitrogen-based fertilizers. The other four management scenarios correspond to the combined management options $1+2+3+4$ and these imply a full rehabilitation of the wastewater network, full coverage of the sewerage system (no cesspits) and a reduction from 60% up to 90% for options 1 and 4. It should be kept in mind that if the management period was extended beyond the year 2015 then a less severe management options (less reduction percentages) would be required.

6. Summary and conclusions

This work focuses on the utilization of lumped-parameter models for the assessment of nitrate contamination of the groundwater of GCJC located in Gaza Strip, Palestine. Groundwater contamination by nitrate is an on-going problem in GCA and the GCJC area due to the disposal of untreated/poorly treated wastewater, leakage of wastewater from the sewerage system, the existence of heavy agriculture in the surrounding areas, and due to the cesspits. There is an emerging need to manage the nitrate contamination problem in the groundwater of the GCJC area and GCA as well. As such, models are useful for reconnaissance studies that precede the implementation of the management options which aim at reducing nitrate concentration in groundwater.

In this paper, two LPMs were developed for the simulation of water table elevation and nitrate concentration. The models utilize monthly time steps and take into consideration all the sources and sinks of water and nitrate in the GCJC area. The main outcomes of the LPMs are the average temporal water table elevation and nitrate concentration along with the mass balance components of water and nitrate. LPMs are simple, easy to understand and develop, and efficiently aid in the analysis of the impact of the management options on the nitrate concentration in groundwater.

In order to demonstrate model usability, a set of management options to reduce nitrate concentration in the groundwater of the GCJC area were proposed and evaluated using the developed LPMs. Four broad management options were proposed and tackled the reduction of nitrate concentration in the lateral inflow, rehabilitation of the wastewater collection system, reduction in cesspit usage, and the restriction on the use of nitrogen fertilizers. In addition, management options that encompass. different combinations from the single management options were considered in the analysis. Different management scenarios corresponding to the different management options were investigated. It was found that individual management options were not effective in meeting the MCL of nitrate. However, the combination of the four single management options with full rehabilitation and coverage of the wastewater collection network along with at least 60% reduction in both nitrate concentration in the lateral inflow and the use of nitrogen-based fertilizers would meet the MCL constraint.

There are limitations that should be considered when developing and utilizing LPMs for simulating nitrate concentrations in groundwater. For instance, there are downsides associated with the use of the linear coefficients to account for the nitrogen cycle in the unsaturated zone. Chiefly, the nitrogen dynamics entail piece wise relationships and this in essence does imply nonlinear relationships. Also, the coefficient values especially after being calibrated may not involve any physical meaning and thus every care should be considered when having simulations beyond the calibration dataset. Another limitation that should be addressed is that the LPMs produce one single nitrate concentration value per time step though in reality this concentration varies spatially. Accordingly, when evaluating the efficacy of the management options, this spatiality in concentration is not addressed though there are areas that do not encounter elevated concentrations while other areas may witness the opposite.

Appendix. List of abbreviations

$\upsilon_{\mathcal{R}}$	relative sensitivity coefficient
A	total area of the model domain
Ara_x	Area for each subdivided polygon for calculation of recharge from rainfall
A_u	Area for each crop type
$\mathrm{BIN}_u(t)$	a binary multiplication factor to account for the months that may receive irrigation water or fertilization (1 or 0)
$C(t)$	average nitrate concentration for the GCJC area with time
C_{Ar}	nitrate concentration in artificial recharge
C_{IN}	average nitrate concentration for a specific source
C_{inj}	the average concentration of nitrate at segment j for the adjacent areas (used for lateral inflow)
C_{Ir}	nitrate concentration in irrigation return-flow
CONS_u	consumption of fertilizer for each crop
C_{ra}	nitrate concentration in rainfall
C_{WL}	nitrate concentration in the leakage of water from the distribution network
C_{WWL}	total nitrogen concentration in the leakage of wastewater
$d_{\mathrm{Irr}u}$	monthly irrigation rate for each crop type "u"
D_{p}	the average depths to the bottom of the aquifer
FERT_u	amount of fertilizers applied for each crop type
$\mathrm{FraNO_3N}$	fraction of nitrogen from cesspits that becomes nitrate
Fra_x	fraction of recharge from rainfall for a specific soil type
GCA	Gaza Coastal Aquifer
GCJC	Gaza City and Jabalia Camp
G_{in}	lateral inflow
G_{o}	lateral outflow
$h(t)$	average groundwater table elevation for the GCJC area with time
h_{o}	water table elevation with reference to the sea level at the beginning of each time step
LPM	lumped-parameter model
MCL	maximum contaminant level
M_{I}	model input
M_{O}	model output
msl	mean sea level
N_{CAPITA}	the generated mass of nitrogen per capita
$\mathrm{NGEN_{CSPT}}$	total mass of nitrogen generated from the cesspits
$\mathrm{NO_3}R_{\mathrm{WL}}$	nitrate from leakage of water
$\mathrm{NO_3CR_{CSPT}}$	nitrate from cesspits
$\mathrm{NO_{3DEN}}$	nitrate lost through denitrification
$\mathrm{NO_{3DO}}$	nitrate lost through domestic groundwater pumping
$\mathrm{NO_3GEN_{CSPT}}$	nitrate mass from cesspits
$\mathrm{NO_3}G_{\mathrm{in}}$	the amount of nitrate carried by lateral inflow
$\mathrm{NO_3}G_{\mathrm{o}}$	nitrate lost through lateral outflow
$\mathrm{NO_{3Irr}}$	nitrate lost through irrigation from groundwater
$\mathrm{NO_3}Q_{\mathrm{A}}$	the amount of nitrate carried by artificial recharge
$\mathrm{NO_3}R$	nitrate entering aquifer with recharge
$\mathrm{NO_3}R\mathrm{Ir}$	nitrate from irrigation return-flow
$\mathrm{NO_3}R\mathrm{ra}$	nitrate from rainfall recharge
$\mathrm{NO_3}R_{\mathrm{WWL}}$	nitrate from leakage of wastewater
$\mathrm{NO_3SURP}$	nitrate from fertilizer surplus
PERCONS	fraction of applied fertilizers that are taken up by plants
PERSERV	fraction of population serviced by the sewerage system
POP	total monthly population living within the study area
PUMPDOM	volume of water pumped for domestic purposes
PWA	Palestinian Water Authority
Q_{Ar}	artificial recharge
Q_{DO}	water consumed monthly for domestic purposes
Q_{Irr}	total monthly volume of water used for irrigation
R	total recharge
ra_x	monthly rainfall depth for each subdivided polygon x
R_{CSPT}	recharge from cesspits
R_{Ir}	recharge from irrigation return-flow
R_{ra}	recharge from rainfall
R_{WL}	recharge from water network leakage
R_{WWL}	recharge from wastewater leakage
SURP	total monthly fertilizer surplus from all land use types and corresponding crops
t	time step number
t_{n}	half-life time of nitrate
US EPA	United States Environmental Protection Agency
v	total crop types
V_{w1}	water volume in the aquifer at the end of each time step

V_{wo} water volume in the aquifer at the beginning of each time step
W_{consm} per capita monthly water consumption
WL the volume of leakage from the water distribution network
WT water table elevation measured from the mean sea level
$WW_{cesspits}$ total wastewater generated from cesspits
WWL total monthly wastewater leakage from the collection network
y total number of subdivided polygons for rainfall-recharge calculations
z total number of discretized segments of the model domain
α_{FERT} fraction for fertilizer
α_{Ir} fraction for irrigation
α_{ra} fraction for rainfall
α_{WL} fraction for water leakage
β_{CSPT} fraction for cesspits
β_{WWL} fraction for wastewater leakage
γ fraction of water that becomes wastewater
δ_{CSPT} recharge fraction of wastewater of cesspit
δ_{Irr} fraction of irrigation return-flow that becomes recharge
ΔM_I change in model input
ΔM_O change in model output
ΔS_N change in the mass of nitrate in the groundwater for each time step
ΔS_W change in the groundwater volume for each time step
δ_{WL} recharge fraction of water leakage
δ_{WWL} recharge fraction of wastewater leakage
λ denitrification rate
ΣQ_{IN} total amount of water that enters the model domain
ΣQ_{OUT} total amount of water that leaves the model domain
Φ average effective porosity
Ω_w water leakage fraction from the distribution network
Ω_{ww} wastewater leakage fraction from the sewerage system

References

Agha, S.R., 2006. Use of goal programming and integer programming for quality management – a case study of Gaza Strip. European Journal of Operational Research 174, 1991–1998.

Al-Agha, M.R., 1997. Environmental management in the Gaza Strip. Environmental Impact Assessment Review 17, 65–76.

Almasri, M.N., Kaluarachchi, J.J., 2004a. Implications of on-ground nitrogen loading and soil transformations on groundwater quality management. Journal of the American Water Resources Association (JAWRA) 40 (1), 165–186.

Almasri, M.N., Kaluarachchi, J.J., 2004b. Assessment and management of long-term nitrate pollution of ground water in agriculture-dominated watersheds. Journal of Hydrology 295, 225–245.

Almasri, M.N., Kaluarachchi, J.J., 2005. Modular neural networks to predict the nitrate distribution in ground water using the on-ground nitrogen loading and recharge data. Environmental Modelling and Software 20 (7), 851–871.

Assaf, S.A., 2001. Existing and the future planned desalination facilities in the Gaza Strip of Palestine and their socio-economic and environmental impact. Desalination 138, 17–28.

Ataie-Ashtiani, B., 2007. MODSharp: regional-scale numerical model for quantifying groundwater flux and contaminant discharge into the coastal zone. Environmental Modelling and Software 22 (9), 1307–1315.

Baalousha, H.M., 2003. Risk Assessment and Uncertainty Analysis in Groundwater Modeling. PhD dissertation, der Rheinisch-Westfälischen Technischen Hochschule Aachen, Germany.

Babiker, I.S., Mohamed, M.A.A., Terao, H., Kato, K., Ohta, K., 2003. Assessment of groundwater contamination by nitrate leaching from intensive vegetable cultivation using geographical information system. Environment International 29, 1009–1017.

Barrett, M., Charbeneau, R., 1997. A parsimonious model for simulating flow in a karst aquifer. Journal of Hydrology 196, 47–65.

Bhumbla, D.K., 1999. Agriculture Practices and Nitrate Pollution of Water. West Virginia University Extension Service. http://www.caf.wvu.edu/~forage/nitratepollution/nitrate.htm (accessed 28.09.08).

Cox, S.E., Kahle, S.C., 1999. Hydrogeology, Ground-water quality, and Sources of Nitrate in Lowland Glacial Aquifer of Whatcom County, Washington, and British Columbia, Canada. USGS Water Resources Investigation Report 98-4195, Tacoma, Washington, 251 pp.

De Santa Olalla, F.M., Dominguez, A., Ortega, F., Artigao, A., Fabeiro, C., 2007. Bayesian networks in planning a large aquifer in Eastern Mancha, Spain. Environmental Modelling and Software 22 (8), 1089–1100.

Desbarats, A.J., 2002. A lumped-parameter model of groundwater influx to a mine adit in mountainous terrain. Water Resources Research 38 (11), 1256, doi:10.1029/2001WR001058.

Farmani, R., Henriksen, H.J., Savic, D., 2009. An evolutionary Bayesian belief network methodology for optimum management of groundwater contamination. Environmental Modelling and Software 24 (3), 303–310.

Freeze, R.A., Cherry, J.A., 1979. Groundwater. Prentice Hall, NY.

Frind, E., Duynisveld, W., Strebel, O., Boettcher, J., 1990. Modeling of multicomponent transport with microbial transformation in ground water. The Fuhrberg case. Water Resources Research 26 (8), 1707–1719.

Gelhar, L.W., Wilson, J.L., 1974. Ground-water quality modeling. Ground Water 12 (6), 399–408.

Hajhamad, L., 2007. Management of Nitrate Contamination of Groundwater using Lumped Parameter Models. MSc thesis, An-Najah National University, Nablus, Palestine.

Hasler, B., 1998. Analysis of environmental policy measures aimed at reducing nitrogen leaching at the farm level. Environmental Pollution 102, 749–754.

Henriksen, H.J., Rasmussen, P., Brandt, G., von Bülow, D., Jensen, F.V., 2007. Public participation modelling using Bayesian networks in management of groundwater contamination. Environmental Modelling and Software 22 (8), 1101–1113.

Joosten, L.T.A., Buijze, S.T., Jansen, D.M., 1998. Nitrate in sources of drinking water? Dutch drinking water companies aim at prevention. Environmental Pollution 102, 487–492.

Kalivarapu, V., Winer, E., 2008. A multi-fidelity software framework for interactive modeling of advective and diffusive contaminant transport in groundwater. Environmental Modelling and Software 23 (12), 1370–1383.

Konikow, L.F., Person, M., 1985. Assessment of long-term salinity changes in an irrigated stream–aquifer system. Water Resources Research 21 (11), 1611–1624.

Kraft, G.J., Stites, W., 2003. Nitrate impacts on groundwater from irrigated-vegetable systems in a humid north-central US sand plain. Agriculture, Ecosystems & Environment 100, 63–74.

Lee, Y.W., Dahab, M.F., Bogardi, I., 1991. Nitrate risk management under uncertainty. Journal of Water Resources Planning and Management 118 (2), 151–165.

Lewis, K.A., Bardon, K.S., April 1998. A computer-based informal environmental management system for agriculture. Environmental Modelling and Software 13 (2), 123–137.

Ling, G., El-Kadi, A., 1998. A lumped parameter model for N transformation in the unsaturated zone. Water Resources Research 34 (2), 203–212.

Mao, X., Prommer, H., Barry, D.A., Langevin, C.D., Panteleit, B., Li, L., 2006. Three--dimensional model for multi-component reactive transport with variable density groundwater flow. Environmental Modelling and Software 21 (5), 615–628.

Matthies, M., Berlekamp, J., Lautenbach, S., Graf, N., Reimer, S., 2006. System analysis of water quality management for the Elbe river basin. Environmental Modelling and Software 21 (9), 1309–1318.

McLay, C.D.A., Dragten, R., Sparling, G., Selvarajah, N., 2001. Predicting groundwater nitrate concentrations in a region of mixed agricultural land use: a comparison of three approaches. Environmental Pollution 115, 191–204.

Meisinger, J.J., Delgado, J.A., 2002. Principles for managing nitrogen leaching. Soil and Water Conservation 6, 485–498.

Mercado, A., 1976. Nitrate and chloride pollution of aquifers: a regional study with the aid of a single-cell model. Water Resources Research 12 (4), 731–747.

Metcalf, Eddy, 2000. Coastal Aquifer Management Program (CAMP): Final Model Report. USAID and PWA, Gaza, Palestine.

Mitchell, R.J., Babcock, R.S., Gelinas, S., Nanus, L., Stansey, E., 2003. Nitrate distribution and sources identification in the Abbotsford-Sumas aquifer, Northwestern Washington State. Environmental Quality 32, 789–800.

Oenema, O., Liere, L.V., Schoumans, O., 2004. Effects of lowering nitrogen and phosphorus surpluses in agriculture on the quality of groundwater and surface water in the Netherlands. Journal of Hydrology 304 (1–4), 289–301.

Palestinian Water Authority, 2006. Environmental Assessment: North Gaza Emergency Sewage Treatment Plant Project. Final Report.

Qahman, M., 2004. Aspects of Hydrogeology, Modeling, and Management of Seawater Intrusion for Gaza Aquifer – Palestine. PhD dissertation, Universite Mohamed V – Agdal Ecole Mohammadia D'ingenieurs.

Santhi, C., Srinivasan, R., Arnold, J.G., Williams, J.R., 2006. A modeling approach to evaluate the impacts of water quality management plans implemented in a watershed in Texas. Environmental Modelling and Software 21 (8), 1141–1157.

Shamrukh, M., Corapcioglu, M.Y., Hassona, F.A.A., 2001. Modeling the effect of chemical fertilizers on ground water quality in the Nile Valley Aquifer, Egypt. Ground Water 39 (1), 59–67.

Shomar, B., 2006. Groundwater of the Gaza Strip: is it drinkable? Environmental Geology 50, 743–751.

Shomar, B.H., Müller, G., Yahya, A., 2005. Geochemical features of topsoils in the Gaza Strip: natural occurrence and anthropogenic inputs. Environmental Research 98, 372–382.

Shomar, B.H., Müller, G., Yahya, A., 2006. Occurrence of pesticides in groundwater and topsoil of the Gaza Strip. Water, Air and Soil Pollution 171, 237–251.

Stournaras, G., 1998. Groundwater and nitrates in Greece – an overview. Environmental Hydrology 6, 4–13.

Tait, N.G., Davison, R.M., Leharne, S.A., Lerner, D.N., 2008. Borehole Optimisation System (BOS) – a case study assessing options for abstraction of urban groundwater in Nottingham, UK. Environmental Modelling and Software 23 (5), 611–621.

Thirumalaivasan, D., Karmegam, M., Venugopal, K., 2003. AHP-DRASTIC: software for specific aquifer vulnerability assessment using DRASTIC model and GIS. Environmental Modelling and Software 18 (7), 645–656.

Turpin, Nadine, Bontems, Philippe, Rotillon, Gilles, Bärlund, Ilona, Kaljonen, Minna, Tattari, Sirkka, Feichtinger, Franz, Strauss, Peter, Haverkamp, Randel, Garnier, Monica, Lo Porto, Antonio, Benigni, Giulia, Leone, Antonio, Nicoletta Ripa, Maria, Eklo, Ole-Martin, Romstad, Eirik, Bioteau, Thierry, Birgand, François, Bordenave, Paul, Laplana, Ramon, Lescot, Jean-Marie, Piet, Laurent, Zahm, F., 2005. AgriBMPWater: systems approach to environmentally acceptable farming. Environmental Modelling and Software 20 (2), 187–196.

UNEP, 2003. Desk Study on the Environment in the Occupied Palestinian Territories. United Nations Environment Programme, Nairobi, Kenya.

U.S. Environmental Protection Agency, 2000. Drinking Water Standards and Health Advisories. U.S. Environmental Protection Agency, Office of Water, 822-B-00-001, 12 pp.

Wolf, J., Beusen, A.H.W., Groenendijk, P., Kroon, T., Rötter, R., van Zeijts, H., 2003. The integrated modeling system STONE for calculating nutrient emissions from agriculture in the Netherlands. Environmental Modelling and Software 18 (7), 597–617.

Wolfe, A.H., Patz, J.A., 2002. Reactive nitrogen and human health: acute and long-term implications. Ambio 31 (2), 120–125.

Yadav, S.N., Wall, D.B., 1998. Benefit-cost analysis of best management practices implemented to control nitrate contamination of groundwater. Water Resources Research 34 (3), 497–504.